

Doubly differential spectra of scattered protons in ionization of atomic hydrogenM. Schulz,¹ A. C. Laforge,¹ K. N. Egodapitiya,¹ J. S. Alexander,^{1,*} A. Hasan,² M. F. Ciappina,³ A. C. Roy,⁴ R. Dey,⁵ A. Samolov,⁶ and A. L. Godunov⁶¹*Department of Physics and LAMOR, Missouri University of Science & Technology, Rolla, Missouri 65409, USA*²*Department of Physics, UAE University, Post Office Box 17551, Al Ain, Abu Dhabi, United Arab Emirates*³*Institute of High Performance Computing, 1 Fusionopolis Way, #16-16, Connexis 138632, Singapore*⁴*School of Mathematical Sciences, Ramakrishna Mission, Vivekananda University, Belur Math 711202, India*⁵*Max Planck Institut für Plasmaphysik, Boltzmannstrasse 2, D-85748 Garching, Germany*⁶*Department of Physics, Old Dominion University, Norfolk, Virginia 23529, USA*

(Received 1 April 2010; published 21 May 2010)

We have measured and calculated doubly differential cross sections for ionization of atomic hydrogen using 75-keV proton impact for fixed projectile energy losses as a function of scattering angle. This collision system represents a pure three-body system and thus offers an accurate test of the theoretical description of the few-body dynamics without any complications presented by electron correlation in many-electron targets. Comparison between experiment and several theoretical models reveals that the projectile-target nucleus interaction is best described by the operator of a second-order term of the transition amplitude. Higher-order contributions in the projectile-electron interaction, on the other hand, are more appropriately accounted for in the final-state wave function.

DOI: [10.1103/PhysRevA.81.052705](https://doi.org/10.1103/PhysRevA.81.052705)

PACS number(s): 34.50.Fa, 34.50.Bw

I. INTRODUCTION

Studies of atomic systems have the important advantage that the underlying fundamental interaction, that is, the electromagnetic interaction, is essentially understood. However, for systems containing more than two mutually interacting particles, the Schrödinger equation is nevertheless not analytically solvable. Wave functions and energy levels of bound states in multielectron atoms can be calculated with satisfactory accuracy using numerical methods such as the multiconfiguration Hartree-Fock procedure [1]. However, systems undergoing a dynamic process, for example, a fragmentation process, represent a serious challenge to theory. One such fragmentation process that has been studied extensively is ionization of atoms by charged-particle impact (for reviews, see, e.g., [2–4]). Relatively recent experiments revealed that the ionization dynamics is not as well understood as assumed previously, even for relatively simple collision systems [5].

In calculations of ionization cross sections, sophisticated modeling of the collision dynamics has to be combined with accurate computations of structural properties of the target atom, especially the wave functions. However, electron-electron correlations in target wave functions may obscure details of the collisional dynamics in ionization cross sections. Besides, even wave functions which provide precise energy levels of bound states, which are often used as a criterion for the quality of the wave function, are not necessarily very accurate for evaluating collision cross sections. The latter tend to be very sensitive to the tails of the wave function at large distances, which do not have a significant impact on the energy levels. Therefore, for the understanding of the basic aspects of the collision dynamics experimental studies of ionization of simple one- or few-electron atoms are crucially important.

Unfortunately, for the most desirable target atom in that regard, that is, hydrogen, cross-section measurements are significantly more difficult than for, for example, noble gas targets. As a result, efforts have focused on ionization of helium and a vast amount of measured data for total and various forms of differential cross sections are available for a variety of projectiles (e.g., [2–13]).

Measured total cross sections for ionization of helium can be reproduced by theory with satisfactory accuracy for a broad range of kinematic conditions. For example, even first-order perturbative models, like the distorted-wave Born approximation, yield good agreement with experiment for proton or electron impact at perturbation parameters η (projectile-charge-to-collision-speed ratio) as large as 0.5 [2,14]. Even better agreement is achieved with models like the continuum-distorted-wave-eikonal-initial-state (CDW-EIS) [15,16] or three-body-distorted-wave (3DW) approaches [17], which account for higher-order contributions in the final-state wave function. However, total cross-section measurements are not ideally suited to test the theoretical description of the few-body dynamics in ionizing collisions. In the integration over the kinematic parameters determining the final state of the collision inaccuracies in the calculation can be averaged out, which could lead to fortuitous agreement with experiment.

A major advancement in the understanding of the ionization dynamics seemed to have been accomplished when measured doubly differential spectra of electrons, ejected by proton impact at energies as small as 100 keV [18], were found to be in good agreement with CDW-EIS calculations (except for fast electrons ejected in the backward direction) [16]. This assessment was reinforced when such spectra were well reproduced by theory, even for 3.6 MeV/amu Au⁵³⁺ ions ($\eta = 4.5$) colliding with helium [19] and heavy target atoms [20]. However, later this optimism was shaken by the comparison between measured and calculated doubly differential cross sections (DDCSs) as a function of ejected electron energy and projectile scattering angle [21,22]. For the very same collision

*Present address: Sensors and Electron Devices Directorate, Army Research Laboratory, Adelphi, Maryland 20783, USA.

system, involving Au⁵³⁺ ion impact, for which the CDW-EIS model nicely reproduced doubly differential electron spectra, the same model was in poor agreement with the measured scattering-angle dependence of the DDCS_{*p*} [22] (the subscript *p* indicates the projectile scattering angle dependence to distinguish these DDCSs from doubly differential ejected electron spectra). Significantly improved agreement was achieved by accounting for the interaction between the projectile and the residual target ion (PT interaction) following the method of Rodriguez and Barrachina [23], but nevertheless major discrepancies remained. There was not even satisfactory agreement for the much simpler system (from a theoretical point of view) 100 MeV/amu C⁶⁺ + He, where $\eta = 0.1$ [22,23].

The discrepancies between the measured and calculated DDCS_{*p*} not only showed that our understanding of the ionization dynamics was less complete than assumed previously, but also provided a first hint that the theoretical problems might be rooted in the description of the PT interaction. Rather strong indications that this is indeed the case were then obtained from fully differential cross-section (FDCS) measurements for ion impact [5,9,24–28] and later for electron impact ionization [29–31]. For a long time, FDCS studies focused on geometries in which only electrons ejected into the scattering plane, spanned by the initial and final projectile momenta, were detected (e.g., [3,11,12,32,33]). There, the experimental data were well reproduced by perturbative approaches at least for large projectile energies (e.g., [34]). Later, sophisticated nonperturbative models for electron impact were developed which treated the entire collision system, including the projectile, fully quantum mechanically (e.g., [35–37]). These calculations achieved impressive agreement with experiment even for collision energies just above the ionization threshold.

For electron ejection outside the scattering plane, the comparison between experiment and theory is much less favorable. In the plane which is perpendicular to the scattering plane and which contains the initial beam axis, to which we refer in the following simply as the perpendicular plane, surprising peak structures were observed which could not be fully explained by theory [5,30,31]. In the case of electron impact, these features could qualitatively be partly reproduced by nonperturbative calculations which account for the PT interaction. However, significant quantitative discrepancies were found, especially at small momentum transfers *q* (difference between initial and final projectile momentum), and perturbative calculations did not even reproduce the peak structures qualitatively at any *q* [31].

For ion impact the discrepancies between experimental and theoretical FDCSs for the perpendicular plane are severe [5]. Here, a major problem is introduced by the large projectile mass, which makes fully quantum-mechanical nonperturbative calculations accounting for the PT interaction much more challenging than for electron impact. First results from a non-perturbative approach, treating the PT interaction semi-classically, were published only very recently [38]. Here too, non-negligible discrepancies to experimental data remain. Otherwise, although promising nonperturbative models without the PT interaction were developed recently [39,40], at present only perturbative approaches accounting for the PT interaction in the final-state wave function can be compared to experiment (e.g., [5,17,41–45]). However, it was pointed out

that the PT interaction, which is contained in the final-state wave function in these models, is only described accurately if at least one collision fragment is far from the other two fragments [46,47], which is not a likely constellation for electron ejection into the perpendicular plane [44,45]. None of these calculations is in satisfactory agreement with measured FDCSs for the perpendicular plane, even at small η . On the other hand, very good agreement with measured data for 100 MeV/amu C⁶⁺ + He was achieved when FDCSs calculated within the first Born approximation (FBA) were convoluted with classical elastic scattering between the projectile and the residual target ion [48] using a Monte Carlo simulation [49].

The present status of studies of ionization of helium by charged particle impact seems to suggest that an accurate description of the PT interaction is a major remaining challenge to theory, especially in perturbative approaches. On the other hand, it is conceivable that the theoretical difficulties are merely due to the relatively complex two-electron initial state of the target atom (see the preceding). For a sensitive test of the theoretical description of the few-body dynamics in ionization, which is not affected by complications due to the presence of passive electrons, experimental data for a pure three-body system, that is, for an atomic hydrogen target, are important. A few data sets of experimental FDCS are available for electron impact (e.g., [50,51]). However, they are restricted to small projectile energies, where significant differences between the cross sections for electron and ion impact are expected [52]. For ion impact, multiple differential measurements are much more difficult than for electron impact. As a result, only experimental total (e.g., [2,53,54]) and singly differential cross sections (e.g., [55]) as well as doubly differential cross sections as a function of the electron energy and ejection angle (DDCS_{*e*}) (e.g., [56]) were reported. Only last year we reported measured DDCS_{*p*} for ion impact [57]. These latter data, which are the most detailed data currently available for a pure three-body system involving ion impact, reinforced the conclusion that the description of the PT interaction represents a major challenge to theory and that the discrepancies between measured and calculated ionization cross sections for helium are not just due to the complications introduced by a many-electron target.

In the present work we have extended the measurements of DDCS_{*p*} as a function of the projectile scattering angle θ_p for fixed energy losses ΔE for 75-keV *p* + H collisions from $\Delta E = 30$ eV to $\Delta E = 50$ eV studied earlier by a new data set for $\Delta E = 53$ eV. The significance of this latter value is that it corresponds to an ejected electron speed v_e equal to the projectile speed v_p . It is well established that at velocities $v_e = v_p$ effects due to the postcollision interaction (PCI) between the outgoing projectile and the ejected electron maximize. Furthermore, the data are analyzed in terms of new theoretical calculations. The comparison between experiment and theory demonstrates that, apart from the PT interaction, the agreement with the experimental data also depends sensitively on an accurate description of PCI.

II. EXPERIMENT

The experimental setup is schematically shown in Fig. 1. A 5-keV proton beam with an energy spread of much less

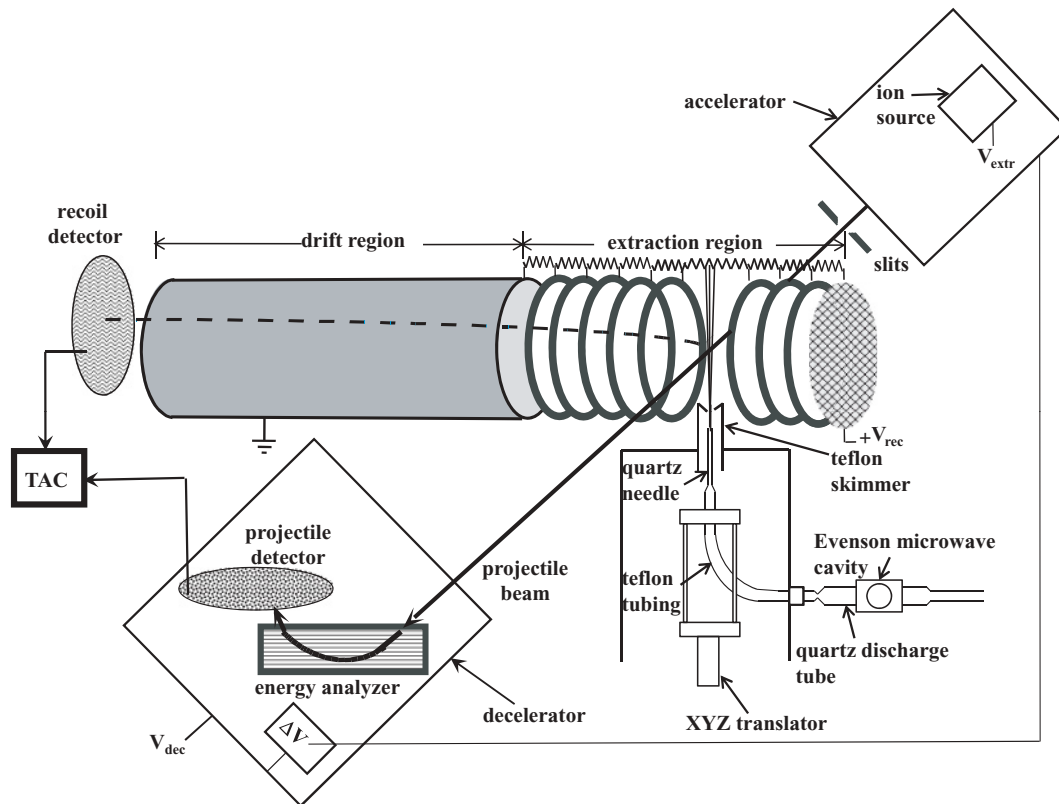


FIG. 1. Schematic diagram of the experimental setup.

than 1 eV was produced with a hot cathode ion source and accelerated to 75 keV. Before passing through the collision chamber the beam was collimated to a size of about 0.15 by 0.15 mm.

The atomic hydrogen target beam was generated by a microwave dissociator using an Evenson cavity resonantly tuned to the frequency of the microwave field of 2.45 GHz [58]. After exiting the quartz discharge tube, the hydrogen gas was guided through Teflon tubing to a Teflon-coated quartz needle. The exit of the needle consisted of a narrow canal 20 mm in length with an inner diameter of 1 mm. The hydrogen escaping from the needle was then collimated by a skimmer, also made out of Teflon, with a diameter of 0.8 mm and located at a distance of about 10 mm from the tip of the needle. The needle was mounted on an XYZ translator so that it could be accurately aligned with the skimmer. The collimation cooled the target gas in the plane perpendicular to the expansion to about 5 K. In the direction of the expansion the beam was cooled due to the pressure gradient between the region inside the needle (≈ 0.4 Torr) and the surrounding region ($\approx 10^{-6}$ Torr). However, here the temperature was significantly higher (≈ 20 K). The hydrogen target beam intersected with the projectile beam at a distance of 20 mm from the skimmer. All components of the target gas assembly were carefully cleaned following the procedures described by Paolini and Khakoo [58].

The recoil ions were extracted perpendicular to the incident projectile beam by a weak, nearly uniform, electric field of 3.6 V/cm. After the electric field region, the recoil ions traveled through a field-free drift region and were detected by a two-dimensional position-sensitive detector. The cooling

of the target together with the position-sensitive detection makes it possible to analyze the momentum of the recoil ions. However, at the time of the experiment the resolution was not optimized yet. Furthermore, since the goal of this study was to measure DDCS_p , which only depend on projectile parameters, momentum-analyzing the recoil ions was not needed.

The scattered projectiles passed through a switching magnet (not shown in Fig. 1) to clean the beam from components which got neutralized by capture from the target gas or the residual gas in the beam line. They were then decelerated by 70 keV, energy analyzed by an electrostatic parallel-plate analyzer [59], and detected by a microchannel-plate detector. The projectile-energy loss was obtained as follows: an offset power supply inside the decelerator terminal provided a voltage ΔV relative to the decelerator ground which was sent to the accelerator terminal. Therefore, after leaving the accelerator, but before the collision, the projectile energy was $(V_{\text{dec}} + V_{\text{extr}} + \Delta V)q$, where the decelerator potential of $V_{\text{dec}} = 70$ kV plus ΔV is equal to the accelerator potential and the ion source extraction voltage V_{extr} was 5 kV. If the projectile suffered an energy loss equal to ΔVq in the collision the projectile energy at the analyzer (i.e., after deceleration) was $V_{\text{extr}}q = 5$ keV. Therefore, the analyzer voltage was kept fixed at a value corresponding to a pass energy of 5 keV. The energy loss of the detected projectiles was thus given by ΔVq . Since the accelerator and decelerator were hard wired together (through the ΔV supply), the ripple on the decelerator and accelerator potential was practically identical and did therefore not affect the energy-loss measurement. This way an energy resolution of 3 eV full width at half maximum (FWHM) was achieved.

The projectile detector was equipped with a two-dimensional position-sensitive wedge-and-strip anode. The entrance and exit slits were very narrow ($\approx 75 \mu\text{m}$) along an axis connecting the slits (the y direction), but long ($\approx 2.5 \text{ cm}$) in the direction perpendicular to that axis (the x direction). Therefore, a broad range of scattering angles (0 to 2 mrad), which were determined by the x position on the projectile detector, could be recorded simultaneously. However, because of the narrow width of the analyzer slits in the y direction, only one energy loss ΔE could be recorded at a time. The scattering angle calibration of the position spectrum was performed using two independent methods. First, a position spectrum was recorded for a fixed ΔE for 75-keV $p + \text{He}$ collisions. The calibration factor was adjusted so that the scattering angle dependence of the DDCS_p measured earlier for this collision system without using a position-sensitive detector [8] was reproduced. In the second method, the channel number of the x position was first calibrated to a position in mm using the known size of the active area of the anode. Next, the distance from the collision region to the decelerator, the length of the decelerator column (where the beam diverges), and the distance from the end of the column to the entrance of the analyzer were measured accurately and the length of the path through the analyzer was calculated from its geometric properties. Using these data and accounting for the divergence in the decelerator column, it is straightforward to convert the x position to scattering angle. The calibration factor obtained from these two methods agreed with each other within 3%. The position resolution of $100 \mu\text{m}$ FWHM resulted in an overall angular resolution (including the divergence of the incident beam) of better than 0.1 mrad FWHM.

The projectile detector signals had to be transformed from the high-voltage plateau of the decelerator to laboratory ground. For the timing signal coming from the back channel plate, this was done by converting the electric signal to a light signal using an optical coupler. The light signal was then detected by a photomultiplier located at ground potential. The three signals from the wedge-and-strip anode, which contain the position information, were converted to optical analog signals, transported to ground potential through fiber optics, and then converted back to electrical signals. The fast timing signals from the back plate of the projectile and recoil-ion detectors served as start and stop signals of a time-to-amplitude converter (TAC) in a coincidence setup. The output of the TAC, that is, the coincidence time, is essentially the time of flight of the recoil ions plus a constant offset due to the constant (because of the fixed energy loss) time of flight of the projectiles.

III. DATA ANALYSIS

In Fig. 2 a typical coincidence time spectrum is shown. Using simple kinematics for motion of a charged particle in a uniform electric field, it is straightforward to show that the time of flight is proportional to the square root of the mass-to-charge ratio of the particle. Ionization of atomic hydrogen and of undissociated molecular hydrogen therefore lead to separate peak structures at about 4.3 and 6.3 μs , respectively, in the coincidence time spectrum. From the intensity ratio between the proton and H_2^+ peaks, we estimate the degree of

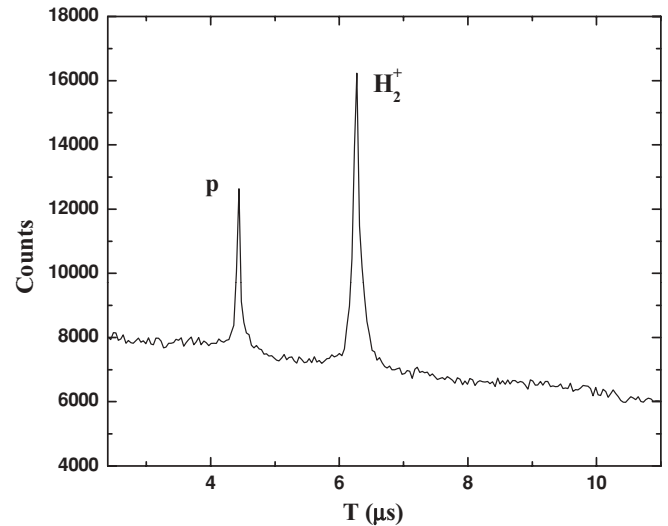


FIG. 2. Projectile-recoil ion coincidence time spectrum for hydrogen gas bombarded by 75-keV protons. The peak labeled p is associated with ionization of atomic hydrogen and the peak labeled H_2^+ is associated with ionization of undissociated molecular hydrogen.

dissociation δ to be about 30% to 40%. About the same value was reached in studies of charge-exchange processes using a similar design for the atomic hydrogen source [60]. This relatively small δ is the price to be paid for a design that makes it possible to perform momentum analysis of the recoil ions (see preceding). Although this feature was not needed in the measurement of the DDCS_p reported here, it is necessary for experiments studying FDCS_p , which are currently in progress.

It should be noted that recoiling protons can also be produced by dissociative ionization of the molecular hydrogen target component. However, the momenta of the fragments are much larger than for protons produced from ionization of atomic hydrogen. As a result, with the relatively weak recoil-ion extraction field used in this experiment, only a very small fraction of the protons produced by dissociative ionization hit the detector. In contrast, protons coming from atomic hydrogen are projected onto the detector with an effective relative solid angle of essentially 100%. In addition, even at the largest scattering angles the DDCS_p for dissociative ionization (which we have measured very recently, but not published yet) are more than an order of magnitude smaller than for ionization of atomic hydrogen. As a result, with the dissociator off we did not observe any indication for a proton time peak at the extraction field of 3.6 V/cm; however, a clear proton peak was found for an extraction field of about 200 V/cm.

For each ΔE a projectile position spectrum was generated with a condition on the proton coincidence time peak. The contributions to the coincident position spectrum from random coincidences underneath the time peak were subtracted as follows: First, the total number of counts in the random spectrum underneath the proton time peak was determined from a spline fit. Then, a second window was set to the left of this peak with a width which was adjusted so that the number of counts in this window was equal to the number of counts underneath the peak obtained from the spline fit. A second projectile position spectrum was generated for this window and subtracted from

the spectrum with the condition on the time peak. Since the x component of the projectile position corresponds to the scattering angle and these spectra were recorded for fixed ΔE , they are directly proportional to the DDCS_p .

To obtain the DDCS_p on an absolute scale the doubly differential position spectra integrated over the projectile solid angle were normalized to singly differential cross sections (SDCSs) as a function of ΔE measured by Park *et al.* [55]. Their SDCSs integrated over ΔE are too large by a factor of 1.8 compared to recommended total cross sections based on a large collection of experimental data [61]. Therefore, the DDCS_p normalized to the SDCS of Park *et al.* were further divided by 1.8. On the other hand, we cannot rule out the possibility that the magnitude of the integrated SDCSs by Park *et al.* are actually more accurate than the recommended total cross sections and this should be kept in mind when comparing to theory. Furthermore, no measured SDCSs are available for $\Delta E > 45$ eV. Up to that energy the data of Park *et al.* divided by 1.8 are exactly a factor of 2 smaller than the

corresponding cross sections for H_2 . At $\Delta E = 50$ and 53 eV, we thus normalized our DDCS_p to half the SDCS for H_2 [62]. This procedure leads to some additional uncertainties in the absolute magnitude of the DDCS_p for these ΔE , especially for 53 eV, which nearly corresponds to $v_e = v_p$. At this matching velocity a step in the SDCS for $p + \text{He}$ collisions was observed [8,21], which is a manifestation of a strong PCI effect. For H_2 , $v_e = v_p$ corresponds to a slightly larger ΔE than for H because of the larger ionization potential. Therefore, in the SDCS for H_2 a step would be expected only at a ΔE larger than 53 eV, while for H 53 eV is very close to the step. This could lead to a slight overestimation of our normalized DDCS_p at 53 eV, which also should be kept in mind when comparing to theory.

IV. RESULTS AND DISCUSSION

In Fig. 3 the DDCS_p are plotted for $\Delta E = 30, 40, 50,$ and 53 eV as a function of the scattering angle θ_p . The data fall off rapidly with increasing θ_p , which is a typical scattering

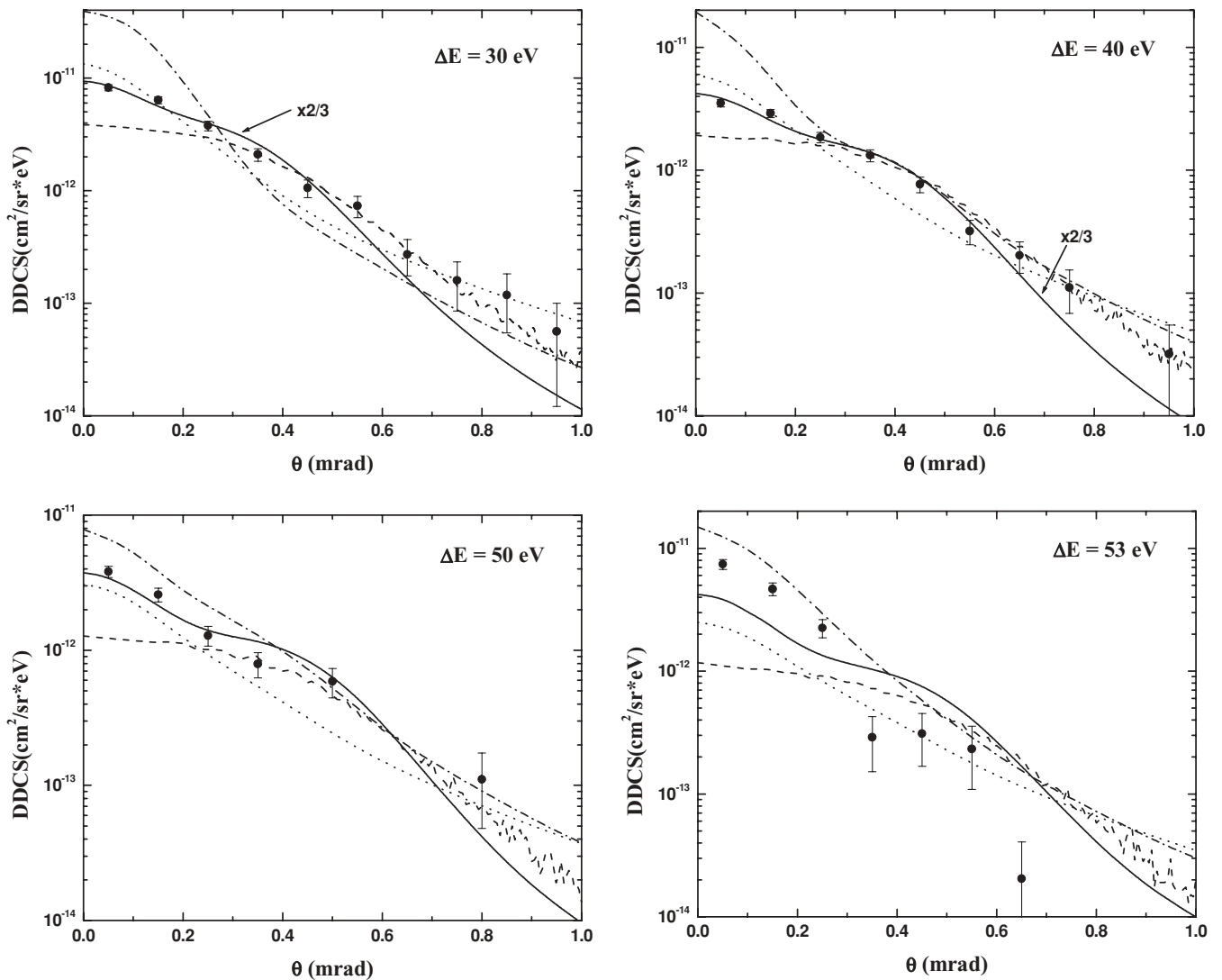


FIG. 3. Doubly differential cross sections for fixed energy losses (as indicated in the legends) as a function of projectile scattering angle. The experimental data are shown as solid circles. The calculations are denoted as follows: dotted curves, CDW-EIS-SC; dashed curves, CDW-EIS-CL; dash-dotted curves, 3C; solid curves, SBA-C.

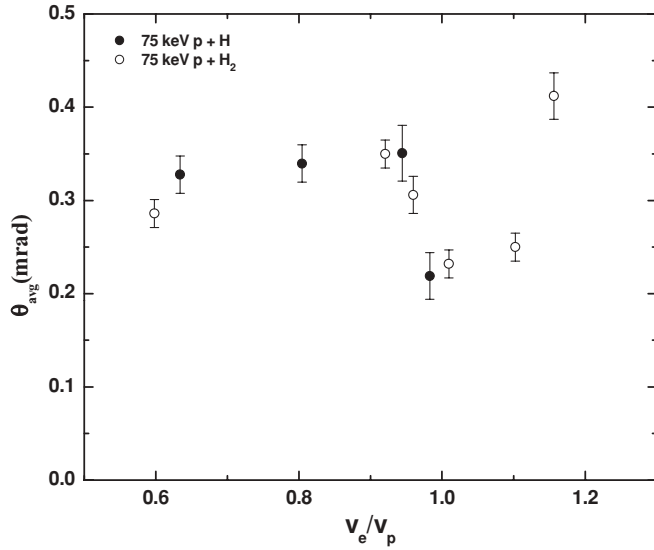


FIG. 4. Average scattering angle in ionization of hydrogen by 75-keV proton impact as a function of the ejected-electron-to-projectile-speed ratio. Open circles, molecular hydrogen target [63]; solid circles, atomic hydrogen target.

angle dependence of cross sections for most processes. At intermediate θ_p (≈ 0.2 - to 0.6 -mrad), the angular dependence exhibits a convex curvature and, at least for $\Delta E = 40$ eV, a shoulder structure can be seen in this region. Earlier, we associated this structure, which is discussed in more detail below, with binary interactions between the projectile and the electron [57].

The rate at which the DDCS_p are dropping is not very sensitive to ΔE up to about 50 eV. However, at 53 eV the width of the DDCS_p suddenly decreases significantly. The same behavior was also observed for ionization of molecular hydrogen [63] and, to a lesser extent, for helium ionization [8,21] by proton impact at the same collision energy. It is illustrated in more detail in Fig. 4, where the average scattering angle $\theta_{\text{avg}} = \int (d^2\sigma/d\Delta E d\Omega_p) \theta_p d\Omega_p / (d\sigma/d\Delta E)$ is plotted as a function of the electron to projectile speed ratio v_e/v_p for atomic (solid circles) and molecular hydrogen (open circles). For atomic hydrogen, the drop in the width of the cross sections near $v_e/v_p = 1$ is quite obvious, but we have no data for $v_e/v_p > 1$ to determine the trend above this matching velocity. On the other hand, for the molecular hydrogen target, a pronounced minimum is observed near $v_e/v_p = 1$. Since PCI is known to maximize in this region [8,21], it is plausible to interpret the sudden narrowing of the DDCS_p at 53 eV as a mutual focusing effect between the outgoing projectiles and the ejected electrons due to the attractive Coulomb interaction. The magnitude of this narrowing is surprising because it is much more pronounced than for a helium target, where only a change of slope, rather than a minimum, in the width of the DDCS_p was observed near $v_e/v_p = 1$ [8,21].

In the following we will compare the experimental DDCS_p to theoretical calculations based on a variety of different models. As mentioned in the Introduction the PT interaction has been identified previously as a factor representing a major challenge to theory [5,9,22,30,57]. Furthermore, the surprising features in the present data described in the preceding para-

graph raise questions as to whether PCI is fully understood. In our analysis of the comparison between theory and experiment we therefore focus on the role of these two interactions.

The dotted curves in Fig. 3 show CDW-EIS calculations, which account for the PT interaction semiclassically in terms of the eikonal approximation assuming a classical straight-line trajectory of the projectile [42]. Higher-order contributions from the projectile-electron interaction are treated in terms of a distortion of the ejected electron wave by the projectile in the final state and in terms of an eikonal phase factor in the initial state. The dashed curves are also based on the CDW-EIS model; however, in this case, the PT interaction is accounted for by convoluting the cross sections calculated without the PT interaction with classical elastic scattering between the heavy particles using a Monte Carlo simulation [48,49,64]. We refer to this model as CDW-EIS-CL to distinguish it from the one which treats the PT interaction within the eikonal approximation (semiclassically), which we call CDW-EIS-SC.

The dash-dotted curves represent calculations based on the three-Coulomb wave (3C) model [65,66], following the numeric implementation of Dey *et al.* [67]. Here, the initial state is described the same way as in the FBA (i.e., a product of an eigenstate of the unperturbed target Hamiltonian and a plane wave for the projectile). The final state is a product of three Coulomb waves describing the three two-particle subsystems (electron-target nucleus, electron-projectile, and projectile-target nucleus) so that both the PT interaction and PCI are treated in the final state. The CDW-EIS and 3C calculations are conceptually similar. In both models, higher-order effects are accounted for in the final state, but not in the operator of the transition amplitude. They differ insofar as the CDW-EIS approach, in contrast to the 3C model, accounts for higher-order contributions in the initial state in addition to the final state. Furthermore, in the 3C method the PT interaction is treated fully quantum mechanically. The solid curves show calculations based on a refinement of the 3C model [68], where the PT interaction has been accounted for not only in the final state, but in the transition operator as well. In [68] it was demonstrated that this model in the limit of higher collision velocities approached asymptotically the second Born approximation (SBA) evaluated in the closure approximation. Since this model not only treats PCI in the same manner as the 3C model, but the PT interaction is included with the same accuracy as in the SBA, we refer to this model as second Born approximation-Coulomb waves (SBA-C).

We presented a comparison between the CDW-EIS-SC and CDW-EIS-CL models and the experimental data for $\Delta E = 30$ to 50 eV earlier [57] and we start our discussion with a summary of the important results of that comparison. Both approaches significantly improve the agreement with the data at large θ_p relative to a CDW-EIS calculation which does not treat the PT interaction at all (CDW-EIS-noPT, not shown in Fig. 3). At small θ_p the CDW-EIS-CL and CDW-EIS-noPT results do not differ much. The CDW-EIS-SC calculations, on the other hand, removes the underestimation of the DDCS_p in the CDW-EIS-noPT model at $\theta_p < 0.2$ mrad. However, it leads to significant discrepancies with the data at intermediate θ_p (≈ 0.2 to 0.6 mrad), where the data are well described by the CDW-EIS-CL and CDW-EIS-noPT calculations. In the latter two, a convex curvature in the theoretical curves is found

in this angular range, in agreement with experiment, which is due to binary interactions between the projectile and the ejected electron [57]. In contrast, the CDW-EIS-SC model leads to a concave curvature, indicating a strong deviation from two-body kinematics due to the PT interaction. Surprisingly, the simple convolution of CDW-EIS with classical elastic scattering overall leads to a better agreement with experiment than treating the PT interaction semiclassically. On the other hand, for $\Delta E = 53$ eV, corresponding to $v_e = v_p$, none of the CDW-EIS calculations are in satisfactory agreement with the data and they do not reproduce the narrowing of the θ_p dependence of the measured DDCS_{*p*} at all.

The comparison of the CDW-EIS calculations to the data, especially at $\Delta E = 53$ eV, shows that apart from the PT interaction PCI also still represents a major challenge to this model. The descriptions of PCI in the 3C and CDW-EIS approaches are very similar and one may therefore not necessarily expect improved agreement with the data for the former model. On the other hand, the fully quantum-mechanical treatment of the PT interaction raises some hope that features due to that interaction are better reproduced by the 3C model. Looking at the data for $\Delta E = 30$ eV, this hope, at a first glance, appears to be disappointed. The discrepancies to experiment are larger than for the CDW-EIS-SC results, essentially in the entire angular range. However, for all other ΔE , the 3C calculations yield significantly better agreement, at least for $\theta_p > 0.2$ mrad. It is particularly interesting that the concave curvature of the 3C curve at $\Delta E = 30$ eV, seen in the CDW-EIS-SC calculations at all ΔE , turns into a convex curvature at 40 and 50 eV, resulting in significantly improved agreement with the experimental data. Perhaps the most remarkable aspect of the 3C results is that they reproduce, apart from possibly slightly overestimating the overall magnitude, the measured DDCS_{*p*} for $\Delta E = 53$ eV fairly well, in sharp contrast to the CDW-EIS models. In particular, the sudden narrowing of the angular distribution of the DDCS_{*p*} relative to $\Delta E = 50$ eV is well reproduced. The 3C model thus reinforces the surprising observation that PCI is more important in $p + \text{H}$ than it is in $p + \text{He}$ collisions.

Except for $\Delta E = 53$ eV, the SBA-C model reproduces the shape of the θ_p dependence of the measured DDCS_{*p*} almost perfectly. At $\Delta E = 30$ and 40 eV there seems to be a discrepancy of about 50% in the magnitude which, however, is not necessarily significant, keeping in mind the uncertainties in the normalization of the data mentioned earlier. Of all calculations presented here, the SBA-C approach yields the best overall agreement with the experimental data for $\Delta E = 30$ to 50 eV. At $\Delta E = 53$ eV, it still fares clearly better than both CDW-EIS calculations, but it does not describe the magnitude and the width of the angular distribution of the DDCS_{*p*} as well as the 3C model.

The comparison between experiment and theory raises several questions, the answers to which could prove important in advancing our understanding of the few-body fragmentation dynamics in simple atomic systems: (i) Why does the classical treatment of the PT interaction within the CDW-EIS approach yield better results than the semiclassical treatment? Since we are obviously dealing with a quantum-mechanical system, this should not be viewed as a success of the CDW-EIS-CL model, but rather as a shortcoming of the CDW-EIS-SC model. (ii) All of the calculations which we presented so far conceptually

contain essentially the same physics and only the technical treatment of the physics is different. Why, then, do they differ so much (up to an order of magnitude in some regions) from each other in the numerical results? (iii) Why do the CDW-EIS and SBA-C calculations not reproduce the strong focusing effect due to PCI at $\Delta E = 53$ eV and why is the 3C calculation much more successful in this regard although it seems to treat PCI conceptually very similarly as CDW-EIS? In the following we try to address these questions by analyzing in more detail to what extent the various higher-order contributions are described in the different models.

We start the discussion of higher-order contributions by pointing out that any interaction included in the final-state wave function is conceptually treated to all orders of perturbation theory. However, since in practice it is not possible to find an exact wave function, not all, or perhaps none, of the higher-order contributions are treated completely and/or accurately. On the other hand, any interaction that is only included in the operator is treated to whatever order the Born series is expanded. The advantage of treating the interaction in the operator is that in principle each order can be treated accurately, unless additional approximations (like, e.g., truncation of the sum over intermediate states or the closure approximation) are employed. An important question then is: What is more important, to include the various interactions to as many orders as possible or to treat specific higher-order contributions (especially the second-order terms) as accurately as possible? The answer to this question may well be different for different interactions.

The 3C wave function is known to be accurate if all three particles are far away from each other, although in some modified versions of the 3C model it is sufficient that one particle is far from the other two particles [46,47]. Furthermore, if the PT interaction leads to a significant deflection of the projectile one would expect that on average all three particles have to approach each other to relatively small distances, at least at large θ_p , because the ejection of the electron requires a relatively close encounter with the projectile. This would suggest that treating the PT interaction within three asymptotic Coulomb waves may result in some inaccuracies (see also [43–45]). On the other hand, if the perturbation η (projectile-charge-to-speed ratio) of the collision is not too large, the magnitude of the various expansion terms usually decreases rapidly with increasing order. Treating the PT interaction within the SBA may therefore be a viable approach.

The framework for higher-order contributions in the projectile-electron interaction, that is, for PCI, is quite different. The PCI interaction distorts the asymptotic of the final-state wave function. This distortion is probably not sufficiently accounted for by the second-order term of the Born expansion. Since the projectile and the electron attract each other, and their relative speed is relatively small, they interact with each other for a long time in the outgoing part of the collision. One would therefore expect terms beyond second order to be quite significant. It is thus probably more appropriate to describe higher-order effects (causing the distortion of the asymptotic of the final state) in the projectile-electron interaction, in contrast to the PT interaction, in terms of a final-state Coulomb wave.

In order to test the preceding hypotheses we analyze the theoretical models presented here in more detail by, starting

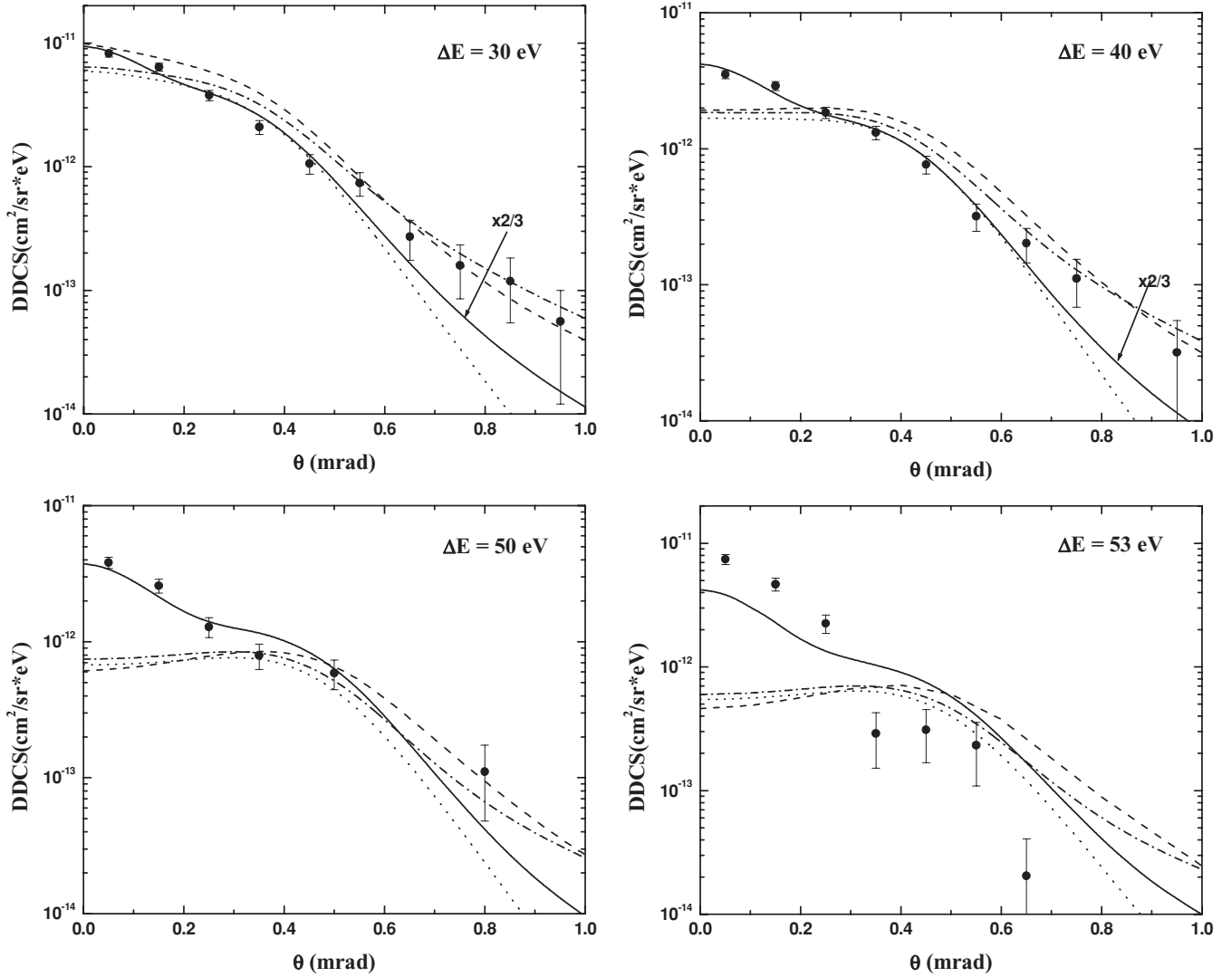


FIG. 5. Same as Fig. 3, but calculations are denoted as follows: dotted curves, FBA; dash-dotted curves, SBA; dashed curves, EA; solid curves, SBA-C.

with the FBA, successively adding the PT interaction and PCI using the respective method of these models. The data of Fig. 3 are shown again in Fig. 5, but this time they are compared to different theoretical curves. The dotted lines represent the FBA results and the dash-dotted lines are SBA calculations. The difference to the SBA-C model is that the projectile is described by a plane wave. Therefore, while the SBA contains the PT interaction in the operator, it does not treat the PCI. As in Fig. 3, the solid curves still represent the SBA-C results.

First, we consider the data for $\Delta E = 30$ eV, which corresponds to the largest $|v_e - v_p|$ of the four energy losses studied here; that is, the influence of PCI should be minimized. Indeed, with decreasing ΔE the SBA results systematically approach both the SBA-C calculation and the experimental data and are in reasonable agreement with the latter at $\Delta E = 30$ eV. On the other hand, results obtained from the eikonal approximation [69] (EA, dashed curves), which roughly corresponds to removing PCI from the CDW-EIS-SC calculations, compare still reasonably well, but less favorable to the measured data than the SBA. This confirms that the PT interaction is more appropriately treated in the operator of the second-order

amplitude than in the final-state wave function. It is interesting to note that the CDW-EIS-CL calculation looks quite similar to the SBA. Apparently, the convolution of CDW-EIS-noPT with classical elastic scattering represents a reasonable simulation (apart from the PCI contributions not included in the SBA) of the SBA. This explains why CDW-EIS-CL yields better results than CDW-EIS-SC.

Next, we consider the influence of PCI on the DDCS_p in the various models. For $\Delta E = 53$ eV, one might expect the PT interaction to play only a minor role compared to PCI because $|v_e - v_p|$ is very small. However, this assumption should be applied cautiously because it cannot be ruled out that the focusing effect due to PCI is at least partly based on an interplay with the PT interaction. To illustrate this point it is helpful to view the ionization process classically in terms of a sequence of collisions between the various particles in the system. The process starts with the primary interaction between the projectile and the electron lifting it to the continuum. As a result of this collision, the two particles now go apart. Classically, any further interaction between the projectile and the electron must be preceded by a redirection of either the projectile

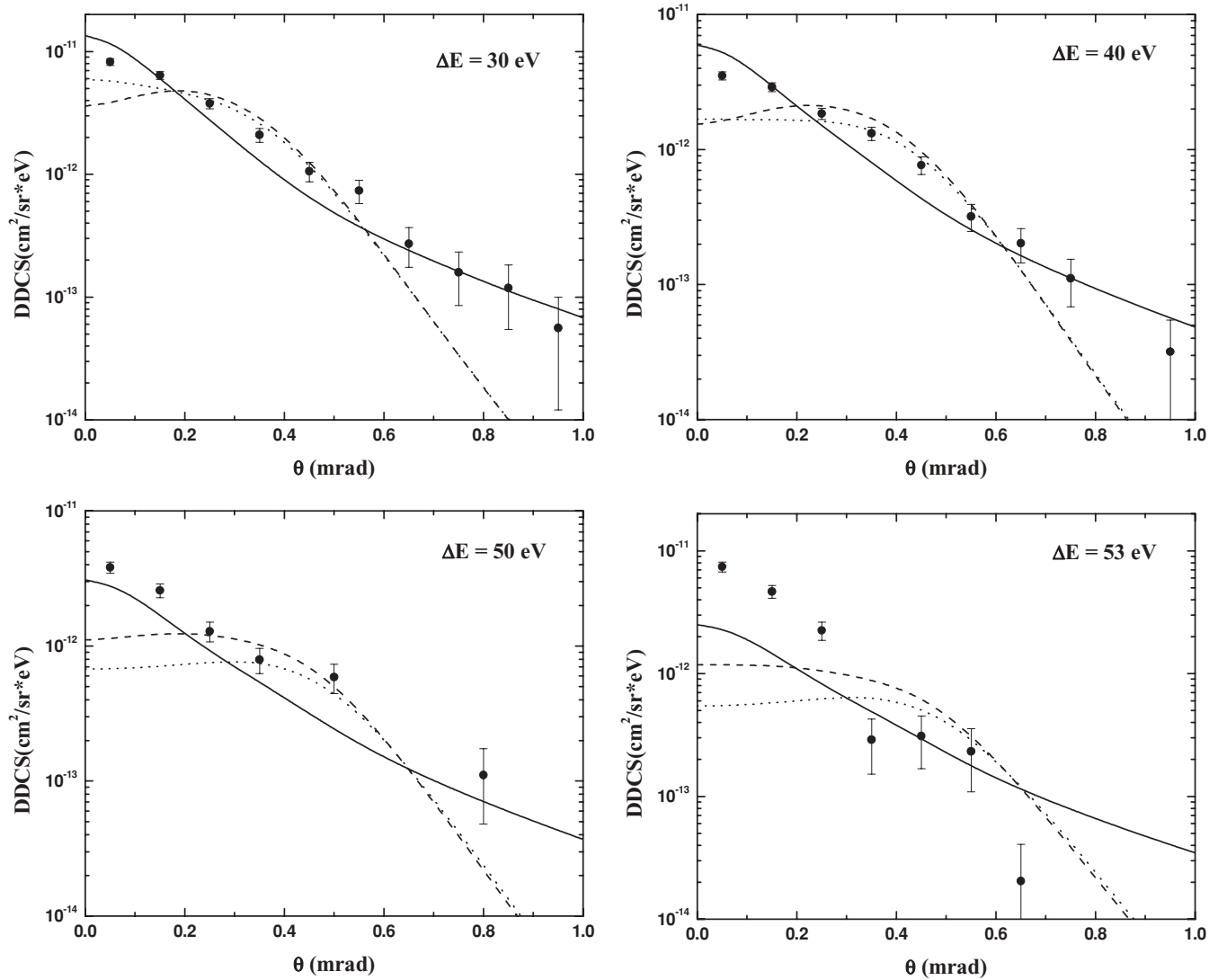


FIG. 6. Same as Fig. 3, but calculations are denoted as follows: dotted curves, FBA; dashed curves, CDW-EIS-noPT; solid curves, CDW-EIS-SC.

or the electron through a collision with the target nucleus. Therefore, the focusing effect may be due to (i) a projectile-electron-electron-target nucleus-projectile-electron (PE-ET-PE) sequence or (ii) a projectile-electron-projectile-target nucleus-projectile-electron collision (PE-PT-PE) sequence. The PE-ET-PE sequence is included in the CDW-EIS-noPT calculation, but the sequence PE-PT-PE is only accounted for by the models treating all interactions (CDW-EIS-SC, 3C, and SBA-C).

To evaluate the contributions of the two sequences described in the preceding paragraph within the CDW-EIS approach, we compare the CDW-EIS-SC (solid curves), CDW-EIS-noPT (dashed curves), and FBA calculations (dotted curves) in Fig. 6. The PE-ET-PE sequence seems to hardly contribute at all to the focusing. Although at $\Delta E = 50$ and 53 eV the intensity at small θ_p is enhanced in the CDW-EIS-noPT calculation compared to the FBA, the width of the angular distribution is not decreased much. Only after the PT interaction is included (CDW-EIS-SC) is a pronounced narrowing compared to the FBA observed. At $\Delta E = 30$ and

40 eV, the intensity at small θ_p even drops below the FBA results if the PT interaction is not accounted for. We conclude that in the CDW-EIS model the focusing due to PCI is predominantly produced by the PE-PT-PE sequence. This could explain why this approach does not reproduce the experimental data as well as the SBA-C calculations. By not treating the PT interaction, involved in this sequence, in the operator (i.e., by not including the second-order contribution completely) the focusing is possibly not described accurately. In fact, it is not even clear whether the CDW-EIS prediction, that the focusing is dominated by the PE-PT-PE sequence, is correct.

The comparison between the experimental data and the various models presented here support our hypothesis that the PT interaction is more appropriately treated within the SBA, but that for describing PCI the 3C approach is more suitable. We can now provide partial answers to some of the questions raised earlier. (i) The classical treatment of the PT interaction within the CDW-EIS model works better than the semiclassical approach because the convolution with classical elastic scattering represents a good simulation of the SBA

(although we do not know why this is the case). (ii) The three theoretical models yield rather different results because the description of the underlying ionization dynamics is quite sensitive to the technical method of treating each interaction. (iii) The question why the 3C model is more successful than the other models in describing the narrowing of the angular distribution of the DDCS_{*p*} at $\Delta E = 53$ eV remains to a large extent unanswered. The lack of success of the CDW-EIS-SC approach in this regard could be related to the semiclassical treatment of the PT interaction.¹ However, the SBA-C model, like the 3C method, also treats the PT interaction fully quantum mechanically. Perhaps the worse agreement of the former with the data is simply due to the large numerical sensitivity of the calculations when $|v_e - v_p|$ becomes very small.

V. CONCLUSIONS

We have presented a thorough analysis of doubly differential ionization cross sections for fixed projectile energies as a function of scattering angle for 75-keV $p + \text{H}$ collisions. The data were compared to three different models, all of them treating all interactions to higher order of perturbation theory. Nevertheless, major differences between the various calculations were found. The SBA-C model is overall in good, but not perfect, agreement with the measured data and the 3C model reproduces the measured cross sections for $\Delta E = 53$ eV reasonably well.

The magnitude of the differences among the calculations, and to some extent also to the experimental data, is surprising because $p + \text{H}$ represents the most simple system for which ionization can occur and theory is not plagued by having to deal with a complicated many-electron state. Especially the discrepancies between the CDW-EIS-SC model and the measured cross sections are disconcerting since the same model yielded excellent agreement with experiment for the more complex collision system $p + \text{He}$ at the same collision energy [23]. On the other hand, the large differences between the various models show that the cross sections are quitesensitive to the details of the description of the ionization dynamics. The

experimental data can therefore be used to check the validity of the approximations used in theory and to determine the most appropriate approaches to account for the higher-order contributions from the various interactions in the collision system.

The comparison between experiment and theory suggests that the projectile-target nucleus interaction is best accounted for in the operator of a second-order term of the transition amplitude. Terms beyond second order in this interaction do not appear to be very significant, at least for this collision system. For the projectile-electron interaction, in contrast, higher-order contributions are probably not negligible and it is therefore more appropriate to treat this interaction in the final-state wave function. The SBA-C model combines the favored methods of including both interactions and as a result yields the best overall agreement with experiment among the models presented here.

The success of the SBA-C model could potentially also be of considerable relevance with respect to the unexpected features observed in the FDSC for electron emission into the perpendicular plane mentioned in the Introduction. Although these observations were interpreted in terms of the PT interaction, calculations which account for it in the wave function were not able to reproduce the experimental data [5]. However, to the best of our knowledge calculations of FDSC for the perpendicular plane based on the SBA-C (or similar) model have not been reported as yet. The significant differences between the calculations presented here along with the success of the SBA-C model demonstrated in this work raise hope that this approach may be able to reproduce these FDSC data as well and thus solve a long-standing puzzle.

An ultimate test of the theoretical description of the few-body dynamics in atomic collisions would be provided by FDSC measurements for $p + \text{H}$ ionization. This requires analyzing the recoil-ion momentum with significantly better resolution than accomplished at the time the experiment reported here was performed. However, since then the recoil-ion momentum resolution has been drastically improved and FDSC measurements are now being initiated.

ACKNOWLEDGMENTS

This work was supported by the National Science Foundation under Grant No. PHY0652519.

¹The importance of treating the PT interaction quantum-mechanically has been pointed out by, e.g., Zapukhlyak *et al.* for the case of capture processes [70].

-
- [1] C. Froese-Fischer, *Adv. At. Mol. Opt. Phys.* **55**, 235 (2008).
 - [2] M. E. Rudd, Y.-K. Kim, D. H. Madison, and J. W. Gallagher, *Rev. Mod. Phys.* **57**, 965 (1985).
 - [3] H. Ehrhardt, K. Jung, G. Knoth, and P. Schlemmer, *Z. Phys. D* **1**, 3 (1986).
 - [4] M. Schulz and D. H. Madison, *Int. J. Mod. Phys. A* **21**, 3649 (2006).
 - [5] M. Schulz, R. Moshhammer, D. Fischer, H. Kollmus, D. H. Madison, S. Jones, and J. Ullrich, *Nature (London)* **422**, 48 (2003).
 - [6] L. C. Tribedi, P. Richard, Y. D. Wang, C. D. Lin, L. Gulyas, and M. E. Rudd, *Phys. Rev. A* **58**, 3619 (1998).
 - [7] E. Y. Kamber, C. L. Cocke, S. Cheng, and S. L. Varghese, *Phys. Rev. Lett.* **60**, 2026 (1988).
 - [8] T. Vajnai, A. D. Gaus, J. A. Brand, W. Htwe, D. H. Madison, R. E. Olson, J. L. Peacher, and M. Schulz, *Phys. Rev. Lett.* **74**, 3588 (1995).
 - [9] N. V. Maydanyuk, A. Hasan, M. Foster, B. Tooke, E. Nanni, D. H. Madison, and M. Schulz, *Phys. Rev. Lett.* **94**, 243201 (2005).
 - [10] A. J. Murray, M. B. J. Woolf, and F. H. Read, *J. Phys. B* **25**, 3021 (1992).
 - [11] G. Stefani, L. Avaldi, and R. Camilloni, *J. Phys. B* **23**, L227 (1990).
 - [12] A. Lahmam-Bennani, A. Duguet, C. Dupré, and C. Dal Cappello, *J. Electron Spectrosc. Relat. Phenom.* **58**, 17 (1992).
 - [13] P. Ashley, J. Moxom, and G. Laricchia, *Phys. Rev. Lett.* **77**, 1250 (1996).

- [14] C. Pan and H. P. Kelly, *Phys. Rev. A* **41**, 3624 (1990).
- [15] D. S. F. Crothers and J. F. McCann, *J. Phys. B* **16**, 3229 (1983).
- [16] P. D. Fainstein, V. H. Ponce, and R. D. Rivarola, *J. Phys. B* **24**, 3091 (1991).
- [17] D. H. Madison, M. Schulz, S. Jones, M. Foster, R. Moshhammer, and J. Ullrich, *J. Phys. B* **35**, 3297 (2002).
- [18] M. E. Rudd, L. H. Toburen, and N. Stolterfoht, *At. Data Nucl. Data Tables* **18**, 413 (1976).
- [19] W. Schmitt, R. Moshhammer, F. S. C. O'Rourke, H. Kollmus, L. Sarkadi, R. Mann, S. Hagmann, R. E. Olson, and J. Ullrich, *Phys. Rev. Lett.* **81**, 4337 (1998).
- [20] R. Moshhammer, P. D. Fainstein, M. Schulz, W. Schmitt, H. Kollmus, R. Mann, S. Hagmann, and J. Ullrich, *Phys. Rev. Lett.* **83**, 4721 (1999).
- [21] M. Schulz, T. Vajnai, A. D. Gaus, W. Htwe, D. H. Madison, and R. E. Olson, *Phys. Rev. A* **54**, 2951 (1996).
- [22] R. Moshhammer, A. N. Perumal, M. Schulz, V. D. Rodriguez, H. Kollmus, R. Mann, S. Hagmann, and J. Ullrich, *Phys. Rev. Lett.* **87**, 223201 (2001).
- [23] V. D. Rodríguez and R. O. Barrachina, *Phys. Rev. A* **57**, 215 (1998).
- [24] D. Fischer, R. Moshhammer, M. Schulz, A. Voitkiv, and J. Ullrich, *J. Phys. B* **36**, 3555 (2003).
- [25] M. Schulz, R. Moshhammer, D. Fischer, and J. Ullrich, *J. Phys. B* **36**, L311 (2003).
- [26] M. Schulz, R. Moshhammer, D. Fischer, and J. Ullrich, *J. Phys. B* **37**, 4055 (2004).
- [27] A. B. Voitkiv, B. Najjari, R. Moshhammer, M. Schulz, and J. Ullrich, *J. Phys. B* **37**, L365 (2004).
- [28] M. Schulz, R. Moshhammer, A. Voitkiv, B. Najjari, and J. Ullrich, *Nucl. Instrum. Methods B* **235**, 296 (2005).
- [29] R. W. van Boeyen, N. Watanabe, J. W. Cooper, J. P. Doering, J. H. Moore, and M. A. Coplan, *Phys. Rev. A* **73**, 032703 (2006).
- [30] M. Dürr, C. Dimopoulou, B. Najjari, A. Dorn, and J. Ullrich, *Phys. Rev. Lett.* **96**, 243202 (2006).
- [31] M. Dürr, C. Dimopoulou, B. Najjari, A. Dorn, K. Bartschat, I. Bray, D. V. Fursa, Z. Chen, D. H. Madison, and J. Ullrich, *Phys. Rev. A* **77**, 032717 (2008).
- [32] H. Ehrhardt, M. Schulz, T. Tekaht, and K. Willmann, *Phys. Rev. Lett.* **22**, 89 (1969).
- [33] A. Lahmam-Bennani, *J. Phys. B* **24**, 2401 (1991).
- [34] P. Marchalant, C. T. Whelan, and H. R. J. Walters, *J. Phys. B* **31**, 1141 (1998).
- [35] T. N. Rescigno, M. Baertschy, W. A. Isaacs, and C. W. McCurdy, *Science* **286**, 2474 (1999).
- [36] I. Bray, *Phys. Rev. Lett.* **89**, 273201 (2002).
- [37] J. Colgan and M. S. Pindzola, *Phys. Rev. A* **74**, 012713 (2006).
- [38] M. McGovern, D. Assafrão, J. R. Mohallem, C. T. Whelan, and H. R. J. Walters, *Phys. Rev. A* **79**, 042707 (2009).
- [39] M. S. Pindzola, F. Robicheaux, and J. Colgan, *J. Phys. B* **40**, 1695 (2007).
- [40] T. G. Lee, S. Yu. Ovchinnikov, J. Sternberg, V. Chupryna, D. R. Schultz, and J. H. Macek, *Phys. Rev. A* **76**, 050701(R) (2007).
- [41] V. D. Rodríguez and R. O. Barrachina, *Phys. Rev. A* **57**, 215 (1998).
- [42] M. F. Ciappina, W. R. Cravero, and M. Schulz, *J. Phys. B* **40**, 2577 (2007).
- [43] D. H. Madison, D. Fischer, M. Foster, M. Schulz, R. Moshhammer, S. Jones, and J. Ullrich, *Phys. Rev. Lett.* **91**, 253201 (2003).
- [44] M. Foster, D. H. Madison, J. L. Peacher, M. Schulz, S. Jones, D. Fischer, R. Moshhammer, and J. Ullrich, *J. Phys. B* **37**, 1565 (2004).
- [45] M. Foster, J. L. Peacher, M. Schulz, D. H. Madison, Z. Chen, and H. R. J. Walters, *Phys. Rev. Lett.* **97**, 093202 (2006).
- [46] Y. E. Kim and A. L. Zubarev, *Phys. Rev. A* **56**, 521 (1997).
- [47] S. Jones and D. H. Madison, *Phys. Rev. A* **62**, 042701 (2000).
- [48] M. Schulz, M. Dürr, B. Najjari, R. Moshhammer, and J. Ullrich, *Phys. Rev. A* **76**, 032712 (2007).
- [49] M. Dürr, B. Najjari, M. Schulz, A. Dorn, R. Moshhammer, A. B. Voitkiv, and J. Ullrich, *Phys. Rev. A* **75**, 062708 (2007).
- [50] J. Röder, H. Ehrhardt, C. Pan, A. F. Starace, I. Bray, and D. V. Fursa, *Phys. Rev. Lett.* **79**, 1666 (1997).
- [51] J. F. Williams, P. L. Bartlett, and A. T. Stelbovics, *Phys. Rev. Lett.* **96**, 123201 (2006).
- [52] H. Knudsen and J. F. Reading, *Phys. Rep.* **212**, 107 (1992).
- [53] W. L. Fite, R. F. Stebbings, D. G. Hummer, and R. T. Brackmann, *Phys. Rev.* **119**, 663 (1960).
- [54] M. B. Shah and H. B. Gilbody, *J. Phys. B* **14**, 2361 (1981).
- [55] J. T. Park, J. E. Aldag, J. M. George, and J. L. Peacher, *Phys. Rev. A* **15**, 508 (1977).
- [56] M. E. Rudd, M. W. Gealy, G. W. Kerby, and Y.-Y. Hsu, *Phys. Rev. Lett.* **68**, 1504 (1992).
- [57] A. C. Laforge, K. N. Egodapitiya, J. S. Alexander, A. Hasan, M. F. Ciappina, M. A. Khakoo, and M. Schulz, *Phys. Rev. Lett.* **103**, 053201 (2009).
- [58] B. Paolini and M. A. Khakoo, *Rev. Sci. Instrum.* **69**, 3132 (1998).
- [59] A. D. Gaus, W. Htwe, J. A. Brand, T. J. Gay, and M. Schulz, *Rev. Sci. Instrum.* **65**, 3739 (1994).
- [60] E. Edgu-Fry, A. Wech, J. Stuhlman, T. G. Lee, C. D. Lin, and C. L. Cocke, *Phys. Rev. A* **69**, 052714 (2004).
- [61] C. F. Barnett, ed., *Atomic Data for Fusion* (Oak Ridge National Laboratory Report No. D6, 1990) [<http://www-cfadc.phy.ornl.gov/redbooks/redbooks.html>].
- [62] M. E. Rudd, Y.-K. Kim, D. H. Madison, and T. J. Gay, *Rev. Mod. Phys.* **64**, 441 (1992), and references therein.
- [63] J. S. Alexander, A. C. Laforge, A. Hasan, Z. S. Machavariani, M. F. Ciappina, R. D. Rivarola, D. H. Madison, and M. Schulz, *Phys. Rev. A* **78**, 060701(R) (2008).
- [64] M. F. Ciappina, T. Kirchner, and M. Schulz, *Comput. Phys. Commun.* **181**, 813 (2010).
- [65] A. L. Godunov, Sh. D. Kunikeev, V. N. Mileev, and V. S. Senashenko, *Zh. Tekh. Fiz.* **53**, 436 (1983).
- [66] M. Brauner, J. S. Briggs, and H. Klar, *J. Phys. B* **22**, 2265 (1989).
- [67] R. Dey, A. C. Roy, and C. Dal Cappello, *Nucl. Instrum. Methods B* **266**, 242 (2008).
- [68] A. L. Godunov, V. A. Schipakov, and M. Schulz, *J. Phys. B* **31**, 4943 (1998).
- [69] R. Dey and A. C. Roy, *Nucl. Instrum. Methods B* **243**, 28 (2006).
- [70] M. Zapukhlyak, T. Kirchner, A. Hasan, B. Tooke, and M. Schulz, *Phys. Rev. A* **77**, 012720 (2008).